^{3}H($\vec{p}$, γ)^{4}He reaction at $E_p = 9.0$ MeV

D. J. Wagenaar, N. R. Roberson, and H. R. Weller
Duke University and Triangle Universities Nuclear Laboratory, Duke Station, Durham, North Carolina 27706

D. R. Tilley
North Carolina State University, Raleigh, North Carolina 27695 and Triangle Universities Nuclear Laboratory, Duke Station, Durham, North Carolina 27706

(Received 15 July 1985)

Angular distributions of cross section and analyzing power were measured for the ^{3}H($\vec{p}$, γ)^{4}He reaction at $E_p = 9.0$ MeV. A transition matrix element analysis including $E1$ and $E2$ terms showed the triplet electric quadrupole ($^3D_2$) amplitude to be larger than predicted by shell model or direct capture calculations. It is shown that the inclusion of $M2$ terms in the T-matrix element analysis does not reduce the $^3D_2$ amplitude, but that the inclusion of $E3$ terms does.

Angular distributions of analyzing power and cross section for the ^{3}H($\vec{p}$, γ)^{4}He reaction have previously been measured at incident proton energies from 6 to 16 MeV.[1] These data were analyzed in terms of the $E1$ and $E2$ transition matrix elements $^1P_1$, $^3P_1$, $^1D_2$, and $^3D_2$, where the notation here denotes the quantum numbers of the incoming partial waves ($^{2S+1}L_J$) in the LS coupling scheme. The results indicated that while the triplet $E1$ amplitude $^3P_1$ accounts for about 1.0 to 1.5% of the total $E1$ cross section, the $^3D_2$ amplitude accounts for as much as 50% of the total $E2$ cross section. Since the electric multipole operators contain only small spin-flip terms, the $S=0$ amplitudes should dominate the $S=1$ amplitudes. This expectation is supported by a recoil-corrected continuum shell model (RCCSM) calculation by Halderson and Philpott,[2] but is in apparent disagreement with the experimental results. As a possible explanation of this result, Halderson and Philpott[2] suggested that the exclusion of other multipoles, in particular $M2$ terms, from the T-matrix analysis might be the reason for obtaining such large values for the $^3D_2$ amplitudes.

The present work reports an improved data set at $E_p = 9.0$ MeV obtained with the two NaI gamma-ray spectrometers at the Triangle Universities Nuclear Laboratory (TUNL). The use of two detectors at symmetric angles on opposite sides of the beam direction made possible the reduction of statistical and systematic errors. As will be seen below, the analysis of the improved data did not change the results of Ref. 1 if only $E1$ and $E2$ radiation are assumed. The effects of adding other multipoles to the analysis will be discussed.

A detailed description of the experimental apparatus has been published elsewhere[3] and only the salient features will be given here. Each gamma-ray spectrometer consists of a 25.4×25.4 cm NaI(Tl) crystal mounted within a well-type plastic scintillating anticoincidence shield. The detectors subtended a solid angle of 33 msr. The target used in this work was a 5 μm tritiated titanium foil containing about 60 μg/cm^2 of tritium. The polarized beams were produced by the TUNL Lamb-shift source and accelerated by an FN tandem. The beam polarization was checked by measuring analyzing powers for the ^{3}H($\vec{p}$, p)^{3}H reaction and comparing the measured results with known values.[4] The results were found to be in excellent agreement with those obtained via the quench-ratio method.[5] Beam polarizations, measured using the quench-ratio method during the course of the experiment, were typically 0.74 ± 0.03.

A typical gamma-ray spectrum is shown in Fig. 1. The spectra were fitted with a standard line shape to determine a centroid and width. The data were then summed over a region which extended from 2.0 widths below the centroid to 1.0 width above it. Background spectra were obtained by bombarding a nontritiated foil and were used to determine that the backgrounds in the peak summing regions were essentially all from the cosmic-ray events in the NaI not rejected by the anticoincidence shield. These backgrounds were subtracted from each peak sum, although their contribution was at most 1% of the sum. Each peak sum was corrected for the accidental coincidences between the NaI crystal and the shield, since these coincidences cause a reduction in the counts in the gamma-ray spectrum. This correction was in all cases less than 1%. The peak sum was also corrected for data acquisition dead time, which was typically 2%.

The analyzing powers $A(\theta)$ were computed from the expression

$$A(\theta) = \frac{(r-1)}{P(r+1)} ,$$

where

$$r^2 = \frac{\mathrm{LU} \times \mathrm{RD}}{\mathrm{LD} \times \mathrm{RU}} .$$

LU(LD) represents the number of counts obtained in the left detector for a spin up (down) beam, RU(RD) the same for the right detector, and P is the beam polarization. If the polarization is not the same for both spin up and spin down beams, as was the case in the present work, the expression for $A(\theta)$ is still dependent only on r and P, although it is somewhat more complicated. As can be seen above, first-order effects due to variations in the integrated charge, target thickness, and detector efficiencies cancel in the r equation and therefore do not appear in the analyzing power expression.

The count rates in both shields and NaI crystals were monitored during the experiment and were kept well below

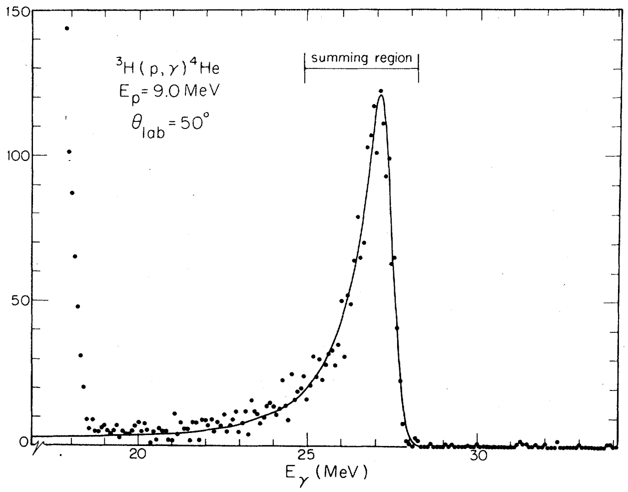

FIG. 1. A typical gamma-ray spectrum obtained with one of the NaI detectors. The summing region shown was taken to be two widths [full width at half maximum (FWHM)] down and one width up from the centroid; the widths and centroids were found from the standard line shape fit.

TABLE I. Experimental and theoretical a_k and b_k coefficients. Errors shown are the statistical uncertainties.

	Present work[a]	Present work[b]	Stanford[c]	RCCSM[d]
a_1	0.223 ± 0.003	0.221 ± 0.004	0.213 ± 0.011	0.21
a_2	-0.966 ± 0.004	-0.986 ± 0.008	-0.954 ± 0.015	-0.98
a_3	-0.238 ± 0.007	-0.238 ± 0.007	-0.216 ± 0.021	-0.21
a_4	-0.008 ± 0.009	-0.020 ± 0.010	-0.010 ± 0.020	-0.01
a_5		-0.010 ± 0.011		
a_6		-0.037 ± 0.014		
b_1	-0.004 ± 0.005	-0.005 ± 0.005	-0.018 ± 0.010	0.000
b_2	0.062 ± 0.003	0.059 ± 0.004	0.080 ± 0.007	0.048
b_3	0.008 ± 0.002	0.010 ± 0.003	0.003 ± 0.006	0.003
b_4	0.002 ± 0.003	0.002 ± 0.003	-0.005 ± 0.007	0.000
b_5		0.001 ± 0.003		
b_6		-0.003 ± 0.004		

[a]Fit through $n=4$.
[b]Fit through $n=6$.
[c]Reference 1.
[d]Reference 2.

values that might cause detector efficiency changes or polarization-dependent dead times. Systematic errors resulting from deviations in the incident beam geometry were calculated. The errors considered included polarization-dependent beam position and incident angle, as well as the effects of a possible misalignment of the center-of-rotation of the detector mounts. In the worst case, no a_k or b_k coefficient was changed by more than a third of the statistical error. In what follows only statistical errors are given.

The angular distribution of cross section is shown in Fig. 2 and is the result of three separate runs. Two of the measurements were made with the two detectors set at equal angles on opposite sides of the beam direction, and the data at each angle were normalized to the integrated beam current. One run was made with one of the detectors serving as a monitor. The solid lines in Fig. 2 are the result of fitting by an expansion of Legendre polynomials given by

$$\sigma_u(\theta) = A_0\left[1 + \sum_{k=1}^{n} a_k Q_k P_k(\cos\theta)\right] ,$$

where the Q_k's are the usual angular attenuation coefficients which correct for the finite geometry effects.[6] The a_k coefficients are given in Table I for $n=4$ and $n=6$. The a_k coefficients obtained from fitting the three individual runs were consistent with those given in Table I.

The angular distribution of cross-section times analyzing power is given in Fig. 3. The solid curve is the result of fitting to an expansion of associated Legendre polynomials

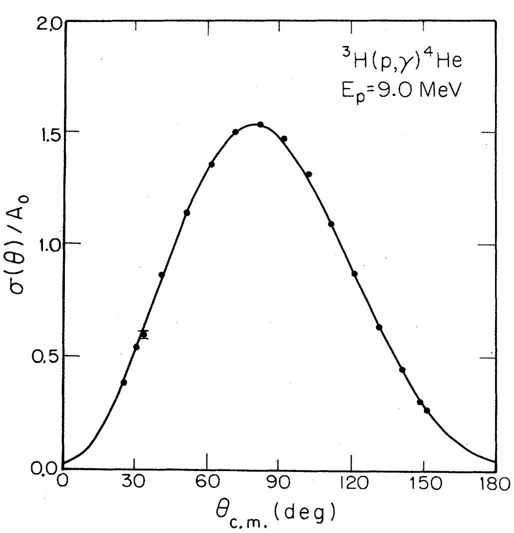

FIG. 2. Angular distribution of cross section in the center of mass coordinate system. Except for one point, statistical errors are smaller than the size of the dots (about 1%). The curve shown is the result of the Legendre polynomial fit through $n=4$.

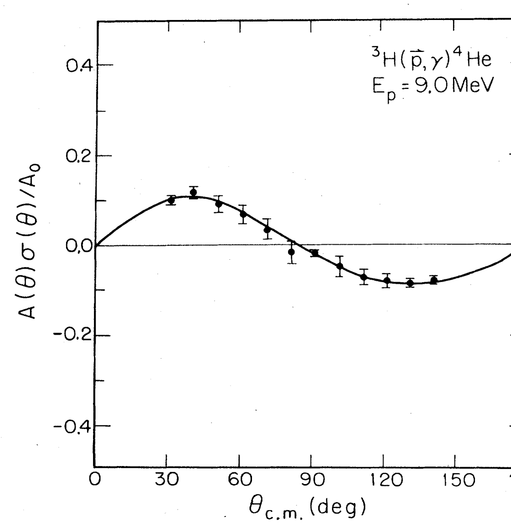

FIG. 3. Angular distribution of analyzing power times the cross section. The curve is the result of the associated Legendre polynomial fit through $n=4$.

TABLE II. Transition matrix amplitudes found for the $^3H(\vec{p},\gamma)^4He$ reaction. The amplitudes are given as percentage of the total cross section.

	Present work	Stanford[a]
$^1P_1$	97.70 ± 0.35	97.9 ± 1.4
$^3P_1$	1.10 ± 0.34	1.5 ± 0.2
$^1D_2$	0.79 ± 0.13	1.1 ± 0.1
$^3D_2$	0.41 ± 0.37	0.5 ± 0.6

[a]From graph in Ref. 1.

given by

$$A(\theta)\sigma_u(\theta) = A_0 \sum_{k=1}^{n} b_k Q_k P_k^1(\cos\theta) \ .$$

The b_k coefficients are given in Table I for $n=4$ and $n=6$. Also given in Table I are the a_k and b_k coefficients taken from the Stanford experiment.[1] For the present work, the a_k coefficients have errors that are approximately 3 times smaller than those obtained previously, while the b_k errors are about 2 times smaller. The a_k and b_k coefficients predicted by the RCCSM calculations of Halderson and Philpott[2] are presented in the last column of Table I and are in good overall agreement with the results of the present work.

The transition matrix element analysis[7] of the improved data set was initially carried out assuming, as did the authors of Ref. 1, only $E1$ and $E2$ radiation. The results are given in Table II as a percentage of the total cross section due to each amplitude. The Stanford results[1] are also shown here. As can be seen, a large $^3D_2$ strength is required to fit both the data sets. The improved accuracy of the present data reduced significantly the error in the extracted $^1P_1$ strength and to a lesser extent that of the $^3D_2$ strength. The uncertainty in the $^3D_2$ strength is still the same size as the strength itself.

As mentioned above, Halderson and Philpott suggested that the inclusion of other radiation amplitudes (specifically $M2$) in the T-matrix element analysis might reduce the large $^3D_2$ strength. The analysis was therefore expanded to include (1) $M2$, (2) $M1$, or (3) $E3$ amplitudes. No combination of T-matrix elements using $E1$ and $E2$ together with either $M1$ or $M2$ gave a fit in which the $^3D_2$ amplitude was reduced and which had an acceptable χ^2. The only T-matrix element analysis which gave a satisfactory fit to the data and had a reduced $^3D_2$ strength was one including $E3$ radiation ($^1F_3$ and $^3F_3$). The results of the best fit ($^3F_3$ set equal to zero) are given in Table III. It should be noted that the $E1$-$E2$ analysis required fourth order in the polynomial expansions, while the $E1$-$E2$-$E3$ fit was extended to sixth order.

TABLE III. Amplitudes found including $E3$ radiation and using terms through sixth order as described in the text. Amplitudes are given as the percentage of the total cross section.

Multipole	T-matrix element	T-matrix amplitude (%)	Direct reaction calculated amplitude (%)
$E1$	$^1P_1$	97.66 ± 0.42	94.3
	$^3P_1$	0.97 ± 0.45	5.2
$E2$	$^1D_2$	0.76 ± 0.08	0.53
	$^3D_2$	0.20 ± 0.32	0.001
$E3$	$^1F_3$	0.54 ± 0.44	8.2×10^{-4}
	$^3F_3$	0.00[a]	1.4×10^{-6}

[a]Best fit when set equal to zero.

A direct capture model calculation[7] was performed in order to investigate the order-of-magnitude of $E3$ contributions. The continuum wave function was calculated using an optical model potential. The bound state single particle wave function was obtained using a Woods-Saxon potential, including a spin-orbit term. The optical model and Woods-Saxon potential parameters were those used by Ward[8,9] for analysis of the $^3He(\vec{n},\gamma)^4He$ reaction. The calculated percentages of σ_t due to the $E1$-$E2$-$E3$ T-matrix elements are shown in the right column of Table III.

The triplet $(S=1)$ terms predicted by this calculation are nonzero due to the inclusion of a spin-orbit term in the potential. As expected, they are dominated by their respective singlet terms for each electric multipole in agreement with our analysis. The amplitude of the $E3$ singlet F term in the direct reaction is three orders of magnitude smaller than the value obtained in the T-matrix analysis.

Despite the improved accuracy of this two-detector measurement, a large $^3D_2$ strength persists in the T-matrix analysis for the $E1$-$E2$ case. The inclusion of $M2$ multipole terms in the T-matrix analysis did not bring the $^3D_2$ amplitude into agreement with the calculations, as was suggested by Ref. 2. The addition of $E3$ radiation to the analysis did lower this spin-flip $E2$ strength, but it gave a singlet F term much larger than expected from a direct reaction calculation. Even further improvement in the data is likely to be needed to clarify the situation. A RCCSM calculation which includes $E3$ effects would also be useful.

This work was supported by the U.S. Department of Energy Director of Energy Research, Office of High Energy and Nuclear Physics, under Contract No. DE-AC05-76ER01067.

[1]G. King, Ph. D. thesis, Stanford University, 1978 (unpublished); see also Ref. 2 below.
[2]D. Halderson and R. J. Philpott, Nucl. Phys. **A359**, 365 (1981).
[3]H. R. Weller and N. R. Roberson, IEEE Trans. Nucl. Sci. **NS-28**, 1268 (1981).
[4]R. A. Hardekopf, P. W. Lisowski, T. C. Rhea, R. L. Walter, and T. B. Clegg, Nucl. Phys. **A191**, 481 (1972).
[5]T. A. Trainor, T. B. Clegg, and P. W. Lisowski, Nucl. Phys. **A220**, 533 (1974).
[6]A. J. Ferguson, *Angular Correlation Methods in Gamma-Ray Spectroscopy* (North-Holland, Amsterdam, 1965).
[7]H. R. Weller and N. R. Roberson, Rev. Mod. Phys. **52**, 699 (1980), and references therein.
[8]L. Ward, Ph. D. thesis, North Carolina State University, 1981 (unpublished).
[9]P. W. Lisowski, Ph.D. thesis, Duke University, 1973 (unpublished).